

# Two-Step Restoration of $SU(2)$ Symmetry in a Frustrated Ring Exchange Magnet

A. Läuchli,<sup>1</sup> J.C. Domenge,<sup>2</sup> C. Lhuillier,<sup>2</sup> P. Sindzingre,<sup>2</sup> and M. Troyer<sup>3</sup>

<sup>1</sup> *Institut Romand de Recherche Numérique en Physique des Matériaux (IRRMA), PPH-Ecublens, CH-1015 Lausanne*

<sup>2</sup> *Laboratoire de Physique Théorique des Liquides, Université P. et M. Curie, case 121, 4 Place Jussieu, 75252 Paris Cedex. UMR 7600 of CNRS*

<sup>3</sup> *Institut für Theoretische Physik, ETH Hönggerberg, CH-8093 Zürich, Switzerland*

(Dated: November 17, 2018)

We demonstrate the existence of a spin-nematic, moment-free phase in a quantum four-spin ring exchange model on the square lattice. This unusual quantum state is created by the interplay of frustration and quantum fluctuations which lead to a partial restoration of  $SU(2)$  symmetry when going from a four-sublattice orthogonal biaxial Néel order to this exotic uniaxial magnet. A further increase of frustration drives a transition to a fully gapped  $SU(2)$  symmetric valence bond crystal.

PACS numbers: 75.10.Jm, 75.40.Mg, 75.40.Cx

Broken symmetries are one of the central paradigms of magnetic ordering, and most antiferromagnetic systems are in Néel phases at low temperatures, characterized by a vectorial order parameter: their sublattice magnetic moment. This order parameter breaks the rotational  $SU(2)$  symmetry of the Hamiltonian and is accompanied by gapless excitations, the Goldstone modes of the broken symmetry [1]. In low-dimensional systems of Heisenberg spins frustrating couplings can drive transitions to gapful  $SU(2)$  symmetric quantum states, where the building blocks are local singlets (in the simplest examples, pairs of spin-1/2 in short-range singlet states). These quantum gapped phases may have long-ranged singlet order and break spatial symmetries of the lattice, called valence bond crystals (VBC) in the following. An even more exotic groundstate, a coherent superposition of all lattice-coverings by local singlets, a state known as a resonating valence bond (RVB) spin liquid, could also be found [2].

Quantum Phase Transitions from Néel ordered phases to quantum gapped phases have been studied for a long time as prototypical examples of quantum phase transitions. The nature of the symmetry breaking Néel phase plays an important role in these scenarios and seems determinant as to whether the adjacent gapped phase will be a VBC or an RVB phase [3]. It was recently shown that the transition from the standard collinear  $(\pi, \pi)$  Néel state to a Valence Bond Crystal phase can actually be an exotic quantum critical point with deconfined excitations [4].

The well-known  $(\pi, \pi)$  Néel state is a uniaxial magnet, with two gapless Goldstone modes, in which  $SU(2)$  is partially broken to  $U(1)$ . More complete  $SU(2)$  breaking schemes do exist, for example in noncollinear magnets with more than two ferromagnetic sublattices or more generally in helicoidal antiferromagnets. In these systems, the order parameter can be described as biaxial (or as a top), the  $SU(2)$  symmetry is completely broken, and there are three Goldstone modes. Chandra and Coleman suggested that in such situations the restoration of

the full  $SU(2)$  symmetry due to the interplay of quantum fluctuations and frustration could possibly occur in two steps: from a biaxial magnet via an intermediate uniaxial *spin nematic* magnet – still with gapless excitations – to a fully gapped paramagnetic phase without  $SU(2)$  symmetry breaking [5, 6]. This speculated spin-nematic phase – first introduced by Andreev and Grishchuk [7] – has *no* net magnetic moment, but nevertheless breaks the  $SU(2)$  symmetry, as the individual spins – albeit disordered – remain correlated in a plane. Up to now this conjectured two-step scenario misses a concrete realization, as it has not been found in the models originally proposed, e.g. the  $J_1 - J_3$  model on the square lattice or various models on the kagome lattice.

In this Letter we present the phase diagram of a frustrated four-spin ring exchange model for  $S = 1/2$  on the square lattice. We show that this model has a four-sublattice orthogonal Néel groundstate with a biaxial order parameter. This groundstate maximizes the square of the vectorial chirality, and appears as a natural “unfrustrated” starting point in the following. Increasing the frustration by a change in the nearest neighbor antiferromagnetic coupling, provides a first realization of the mechanism speculated by Chandra and Coleman [5]. Based on the analysis of spin-resolved spectra, the transition from a biaxial to a uniaxial magnet – accompanied by the reduction from three Goldstone modes in the biaxial magnet to only two Goldstone modes in the uniaxial one – is highlighted. Upon a further increase in the frustration all spin excitations become gapped and the system enters a (staggered) Valence Bond Crystal phase.

The model Hamiltonian with spin  $S = 1/2$  reads:

$$H = J \sum_{\langle i,j \rangle} \mathbf{S}_i \cdot \mathbf{S}_j + K \sum_{[i,j,k,l]} (P_{i\dots l} + P_{i\dots l}^{-1}). \quad (1)$$

$P_{i\dots l}$  is the cyclic permutation of the 4 spins sitting on a square plaquette, and the two sums run respectively over the nearest neighbor bonds and the plaquettes of the square lattice. We parametrize the couplings by  $J = \cos \theta$  and  $K = \sin \theta$ . The explicit expression of the 4-spin

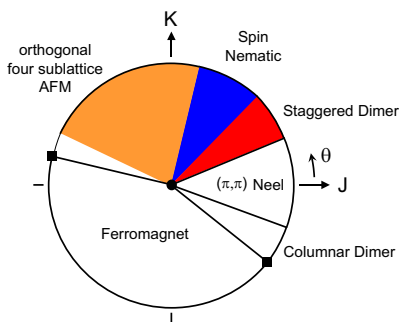


FIG. 1: (Color online) Schematic phase diagram of the cyclic four-spin exchange Hamiltonian (1) on the square lattice as a function of the parameter  $\theta$ .

permutation operators in terms of spin-1/2 operators can be found in Ref. [8].

Interest in the present model has arisen 15 years ago in an early attempt to describe the magnetism of the cuprates [9, 10]. It has been shown very recently to be relevant to describe the high-energy spin waves dispersion of  $\text{La}_2\text{CuO}_4$  [11]. In this material, the four-spin ring exchange term is significant, but still rather small compared to the usual Heisenberg term [12]. Here we study this model in a broader range of parameters. Recent studies of the Hamiltonian (1) on a two-leg ladder have provided evidence for a number of unconventional phases [13, 14]. Of particular relevance for the present work is the appearance of a short range ordered, gapped phase with dominant *vector chirality* correlations in a large region of the phase diagram.

Our results on the overall phase diagram obtained by large scale exact diagonalizations of systems up to  $N = 40$  spins are summarized in Fig. 1. Adjacent to the well established Néel phase around  $J = 1$ ,  $K = 0$ , we find two VBC phases, a staggered dimer phase for positive  $K$  and a columnar dimer phase for negative  $K$ . For negative  $K$  we further find a large ferromagnetic region. These phases for  $K < 0$  are analogous to those observed in a related  $XY$ -like model, amenable to Quantum Monte Carlo simulations [15]. The emphasis of the present paper is on three of the phases found for  $K > 0$ : the coplanar orthogonal antiferromagnet, the spin-nematic state and the staggered dimer VBC. A detailed discussion of the whole phase diagram will be presented in a forthcoming article [16].

*The orthogonal four-sublattice AFM* — Let us start the discussion with a state which has a simple classical interpretation. The cyclic exchange term  $K$  contains both four-spin couplings and two-spin exchange terms. For  $J = -2$  and  $K = 1$  ( $\theta \approx 0.85\pi$ ), the effective nearest neighbor exchange coupling is vanishing [8]. Classical and semiclassical reasonings then predict an orthogonal four-sublattice AFM [9, 10], as shown in Fig. 2a). It could be remarked that this state minimizes the  $SU(2)$  and lat-

$\mathbf{k}$	$\mathcal{R}_{\pi/2}$	$\sigma$	(A)	(B) $N = 8p$	(B) $N = 8p + 4$
$(0, 0)$	1	1	✓	✓	
$(0, 0)$	-1	1	✓		✓
$(\pi, \pi)$	1	1	✓		✓
$(\pi, \pi)$	-1	1	✓	✓	
$(0, \pi), (\pi, 0)$	0	1	✓		

TABLE I: Irreducible representations of the square lattice space symmetry group appearing in the tower of states of the orthogonal Néel state (A) and the spin-nematic state (B) respectively.  $\mathbf{k}$  denotes the momentum,  $\mathcal{R}_{\pi/2}$  the  $90^\circ$  rotation around a site, and  $\sigma$  the site-based reflection along the x or y axis.  $N$  is the number of sites of the sample.

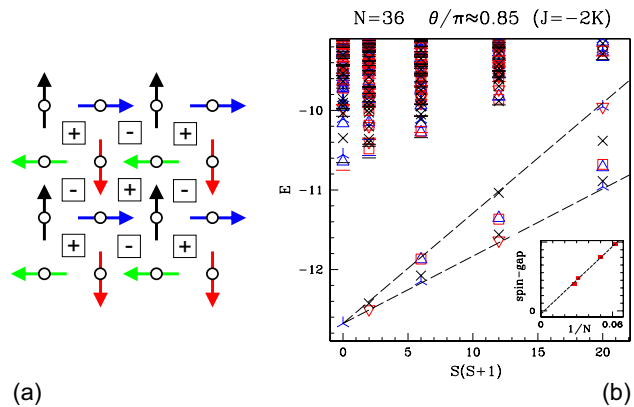


FIG. 2: (Color online) (a) The orthogonal Néel state. It has a coplanar, four-sublattice structure. The vector chirality on a plaquette possesses a  $(\pi, \pi)$  structure. (b) Tower of states in the orthogonal four-sublattice Néel state for  $J = -2$ ,  $K = 1$  ( $\theta \approx 0.85\pi$ ). The eigenstates between the dashed lines form the groundstate manifold of the orthogonal Néel state. Taking into account exact degeneracies of some of the states we find  $2S + 1$  low-lying levels in each spin- $S$  sector, consistently with a complete  $SU(2)$ -symmetry breaking order parameter. Inset: finite size scaling of the spin gap, indicating a vanishing spin gap in the thermodynamic limit.

tice symmetric Hamiltonian:  $\mathcal{H}' = -\sum_i \mathcal{C}_i^2$ , where  $\mathcal{C}$  is the vectorial chirality on an elementary plaquette:

$$\mathcal{C} = \mathbf{S}_1 \wedge \mathbf{S}_2 + \mathbf{S}_2 \wedge \mathbf{S}_3 + \mathbf{S}_3 \wedge \mathbf{S}_4 + \mathbf{S}_4 \wedge \mathbf{S}_1. \quad (2)$$

Interestingly this Hamiltonian is rather close to our model Eq. (1) in the region  $J = -2$ ,  $K = 1$ .

We now turn to the  $S = 1/2$  fully quantum case, where the presence of the orthogonal Néel state has not yet been shown explicitly. We investigate the nature of the collective ground-state with a spectroscopic method which relies on the analysis of symmetries and scaling of the low lying levels of the exact spectra of the Hamiltonian (1) (called Quasi Degenerate Joint States (QDJS) in the following) [17, 18]. These QDJS embody the dynamics and symmetry of the order parameter of the orthogonal Néel state. As it is a biaxial magnet, its order parameter is a *quantum top*. The leading term of the free dynamics of

a quantum top is proportional to the square of the total spin of the sample  $S$ : its effective spectrum involves  $(2S+1)$  distinct eigenstates in each  $S$  sector, with eigenvalues scaling as  $S(S+1)/N$ .

Fig. 2b) indeed displays such a tower of low lying levels well separated from the other excitations. The symmetries of the QDJS (displayed in Tab. I) are those predicted by the ab initio symmetry analysis; three soft modes at  $(0, \pi)$ ,  $(\pi, 0)$ ,  $(\pi, \pi)$  signal the full symmetry breaking of  $SU(2)$ . The finite size scaling of the QDJS is regular and as expected, the tower of states collapse to the ground-state as  $1/N$  (Inset in Fig 2b) and [16]). Long wavelength quantum fluctuations, estimated in a spin wave approach, lead to a reduction of  $\sim 30\%$  of the sublattice magnetization the thermodynamic limit. The real-space spin correlations as well as the vector chirality correlations are in perfect agreement with these results. Based on the analysis of the exact spectra and finite size scaling of the orderparameters we believe that the four-sublattice Néel phase is stable for  $0.4\pi \lesssim \theta \lesssim 0.9\pi$ .

*The spin-nematic phase* — Frustrating the four-sublattice orthogonal state by increasing  $J$  induces a drastic modification of the low lying spectrum of Eq. 1, which evolves towards the typical behavior of Fig. 3b). The  $1/N$  finite size scaling of this tower of states proves that this phase breaks  $SU(2)$  symmetry [Inset of Fig. 3b)]. But the QDJS which display only one level in each  $S$  sector, embed the dynamics of a rigid rotator: the magnet is a uniaxial magnet, i.e.  $SU(2)$  is only broken down to  $U(1)$ . One observes an enlargement of the spatial symmetry of the order parameter (see column (B) of Table I), incompatible with a standard  $(\pi, \pi)$  antiferromagnet, but consistent with a staggered long range order in the vectorial chirality (2). This is confirmed by the behavior of the correlations in the bond chirality (defined as  $\vec{V}(i, j) = \langle \mathbf{S}_i \wedge \mathbf{S}_j \rangle$ ) shown in Fig. 3a). On the other hand the finite size scaling of the spin-spin correlations points to a wiping out of the sub-lattice magnetization by long wave-length quantum fluctuations. Such a state is therefore a  $p$ -spin-nematic state [5, 6, 7], characterized by the absence of any sublattice magnetic moment  $\langle \mathbf{S}_i \rangle = 0$ , and by the presence of a pseudo-vectorial order parameter  $\vec{V}(i, j) \neq 0$ .

The partial restoration of the  $SU(2)$  symmetry when going from the four-sublattice orthogonal state to the nematic state can be tracked by plotting the relative motion of the different symmetry-breaking levels within the tower of QDJS while lowering  $\theta$ . The energy differences displayed in Fig. 4 show how all but *one* level for each spin sector evaporate once  $\theta/\pi \lesssim 0.5$ . Since the symmetry group of the orthogonal four-sublattice antiferromagnet is contained in the symmetry group of the spin-nematic state we might expect the transition between the two states to be a continuous quantum phase transition, although this remains an open problem.

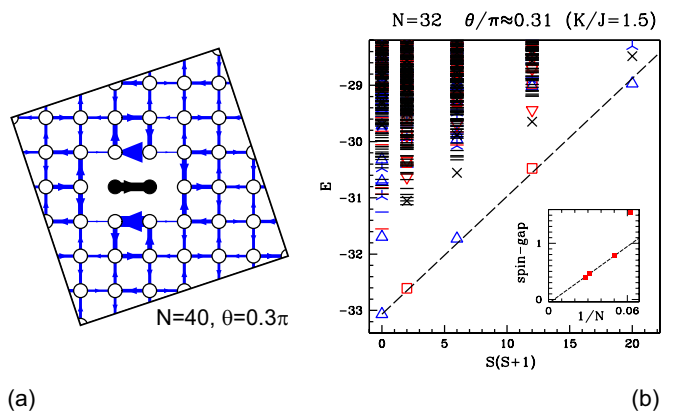


FIG. 3: (Color online) (a) Real space vector chirality correlations  $\langle [\mathbf{S}_0 \wedge \mathbf{S}_1]^z [\mathbf{S}_i \wedge \mathbf{S}_j]^z \rangle$  for a  $N = 40$  sample in the spin-nematic phase at  $\theta = 0.3\pi$ . The black bond denotes the oriented reference bond. The width of the lines is proportional to the correlation strength. (b) Tower of states in the spin-nematic state. Inset: finite size scaling of the spin gap, indicating a vanishing spin gap in the thermodynamic limit.

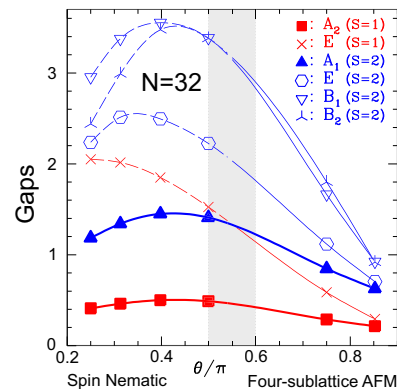


FIG. 4: (Color online) The evolution of the finite size spectral gaps within the QDJS of the orthogonal Néel state on a  $N = 32$  sample. The bold lines denote levels which remain in the QDJS of the spin-nematic state. The other levels detach from the QDJS as  $\theta \lesssim \pi/2$ .

The finite size scaling of the order parameter indicates that the phase should at least exist in the range of parameters  $0.25 \lesssim \theta/\pi \lesssim 0.4$ . The accuracy in the determination of the boundaries cannot be made better on the basis of exact diagonalizations.

*The staggered dimer VBC phase* — Once the nematic state has been destabilized by even stronger frustration we find evidence for a VBC state with a staggered dimer structure. We consistently see an increase of the staggered dimer structure factor for all system sizes considered. The real-space dimer correlations for an  $N = 36$  sample are shown in Fig. 5a). These correlations show a clear staggered pattern and they converge to a finite value at the largest distances. Another strong argument in favor of a staggered dimer phase is the presence of 4

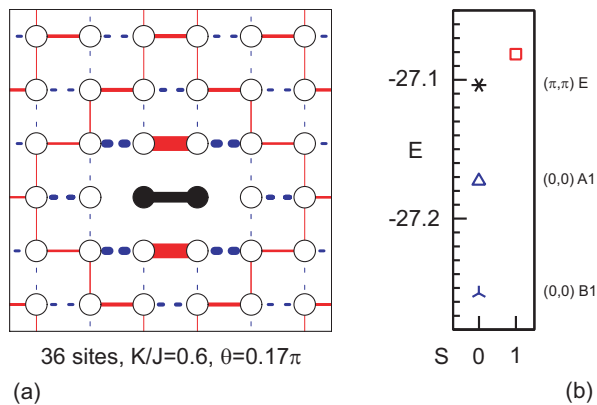


FIG. 5: (Color online) Staggered Valence Bond Crystal phase: (a) Dimer correlations in the groundstate of a 36 site sample at  $\theta \approx 0.17\pi$ . Full, red (dashed, blue) lines denote negative (positive) correlations. The line width is proportional to the correlation. (b) Low energy spectrum of a 36 sites sample in the same phase. The required four singlets (the singlet at  $(\pi, \pi)$  marked with a star is two-fold degenerate) with the correct quantum numbers corresponding to a staggered VBC are found below the first triplet.

singlets which will form the fourfold degenerate ground-state manifold in the thermodynamic limit, as shown in Fig. 5b). We find two distinct singlets at momentum  $(0, 0)$  and a doubly degenerate singlet at  $(\pi, \pi)$ . The symmetry properties of these singlets precisely correspond to those expected for a staggered dimer phase. We note that these findings are in line with earlier work which proposed a staggered dimer phase in a cyclic exchange model on the square lattice [10] and recent studies of a two leg ladder [13, 19].

*Conclusion*— A thorough examination of the low lying spectrum of the ring exchange Hamiltonian on the square lattice revealed how a biaxial magnet may be driven to an uniaxial spin-nematic phase through the interplay of frustration and quantum fluctuations. These fluctuations drive the disappearance of the net magnetic moment of the planar orthogonal four-sublattice state, the spins disorder in the spin plane, the associated Goldstone mode acquires a gap, but nevertheless in a finite range of parameters the plane of spins remains locked. To our knowledge, this is the first clear demonstration of the existence of such a phase in a two-dimensional quantum magnet. At last, increasing again the frustration, the  $SU(2)$  symmetry is completely restored, a spin gap opens simultaneously with the collapse in the  $S = 0$  sector of the four levels leading to the spatial staggered VBC. This is one realization of the two-step restoration of symmetry speculated some years ago by Chandra and Coleman [5].

In some aspects, such as spin susceptibility and thermodynamic properties, the spin nematic phase is not different from a standard Néel phase [7]. But the absence of long range order in ordinary spin-spin correlation functions implies that such systems – although ordered – do

not display a Bragg peak with unpolarized neutrons. Due to the pseudo-vectorial nature of the order parameter, the NMR pattern of the nematic state is different from that of an ordinary Néel phase (different selection rules), providing a clear experimental signature of this phase. It might, however, be obscured by a phenomenon not addressed in this paper, which is the sensitivity to disorder and impurities: disorder might be able to locally pin the spins in the transverse plane leading to a novel type of spin glass.

We acknowledge very interesting discussions with C. Berthier and G. Misguich and R.R.P. Singh. A.L. acknowledges support by the Swiss National Fund and the CNRS. Computations were performed at the LRZ München, the CSCS Manno and at IDRIS Orsay.

- 
- [1] A. Auerbach, *Interacting electrons and Quantum Magnetism*, Springer Verlag, (1994).
  - [2] G. Misguich and C. Lhuillier, cond-mat/0310405. In *Frustrated spin systems*, H. T. Diep, ed., World-Scientific, (2005).
  - [3] S. Sachdev, *Rev. Mod. Phys.* **75**, 913 (2003); *Lect. Notes Phys.* **645**, 381 (2004), cond-mat/0401041.
  - [4] T. Senthil *et al.*, *Science* **303**, 1490 (2004); T. Senthil *et al.*, *Phys. Rev. B* **70**, 144407 (2004).
  - [5] P. Chandra and P. Coleman, *Phys. Rev. Lett.* **66**, 100 (1991).
  - [6] A.V. Chubukov, *Phys. Rev. B* **44**, 5362 (1991).
  - [7] A. F. Andreev and I. A. Grishchuk, *Sov. Phys. JETP* **60**, 267 (1984).
  - [8] M. Roger, J.H. Hetherington, and J.M. Delrieu, *Rev. Mod. Phys.* **55**, 1 (1983).
  - [9] M. Roger and J.M. Delrieu, *Phys. Rev. B* **39**, 2299 (1989); M. Roger and J.H. Hetherington, *Phys. Rev. B* **41**, 200 (1990).
  - [10] A. Chubukov *et al.*, *Phys. Rev. B* **45**, 7889 (1992).
  - [11] R. Coldea *et al.*, *Phys. Rev. Lett.* **86**, 5377 (2001); A.A. Katanin and A.P. Kampf, *Phys. Rev. B* **66**, 100403 (2002); *Phys. Rev. B* **67**, 100404 (2003); P. Sengupta *et al.*, *Phys. Rev. B* **66**, 144420 (2002).
  - [12] The ring-exchange Hamiltonian used in fitting the experiments on  $\text{La}_2\text{CuO}_4$  is somewhat different from our model Hamiltonian. Restricting the comparison to only genuine four-spin terms,  $K \approx 1/16J$  in these materials.
  - [13] A. Läuchli *et al.*, *Phys. Rev. B* **67**, 100409 (2003).
  - [14] T. Hikihara *et al.*, *Phys. Rev. Lett.* **90**, 087204 (2003).
  - [15] A. W. Sandvik *et al.*, *Phys. Rev. Lett.* **89**, 247201 (2002).
  - [16] A. Läuchli, J.C. Domenge, P. Sindzingre, C. Lhuillier and M. Troyer, in preparation.
  - [17] P.W. Anderson, *Phys. Rev.* **86**, 694 (1952); and *Basics Notion of Condensed Matter Physics*, p.44-47, Addison-Wesley (1984).
  - [18] B. Bernu *et al.*, *Phys. Rev. B* **50**, 10048 (1994). C. Lhuillier, cond-mat/0502464.
  - [19] T. Momoi *et al.*, *Phys. Rev. B* **67**, 174410 (2003); V. Gritsev *et al.*, *Phys. Rev. B* **69**, 094431 (2004); P. Lecheminant and K. Totsuka, *Phys. Rev. B* **71**, 020407 (2005).